PHYSICAL REVIEW B VOLUME 26, NUMBER 8 15 OCTOBER 1982

Electronic structure of a hydrogen impurity in nickel with the use of the linear combination of atomic orbitals method

P. G. Rudolf and R. C. Chaney
Department of Physics, University of Texas at Dallas, Richardson, Texas 75080
(Received 17 August 1981; revised manuscript received 2 February 1982)

The method of linear combination of atomic orbitals has been utilized to perform a first-principles calculation of the electronic states of a hydrogen defect in a nickel cluster. The Coulomb and exchange potential for a perfect crystal is curve fitted using a superposition of functions centered about each atom. These functions are then placed at each of the atoms in the cluster to construct the cluster potential. Results are presented for pure nickel clusters consisting of a central atom with five surrounding shells of atoms (79) and with three shells of atoms (43). The five-shell results compare favorably with a perfect crystal density of states and with other cluster calculations. Mulliken population analysis is utilized to examine the surface states. A calculation of the electronic states of a central hydrogen atom surrounded by three shells of nickel atoms (38 Ni atoms) is performed. The density-of-states results are compared with the density of states corresponding to a perfect crystal of nickel hydride and with other cluster calculations.

I. INTRODUCTION

The electronic structure of perfect crystals has generally been computed with the use of methods which take advantage of the translational symmetry of the crystal. In such situations one may require that the wave function obey Bloch's theorem and reduce the size of the secular equation to manageable proportions. Many of the interesting problems of solid-state physics occur, however, in situations where this translational symmetry breaks down. Examples of this include interfaces, the surface of solids, and locations of impurities or defects. An application of the method of linear combinations of atomic orbitals (LCAO) which has achieved a great deal of success recently upon impurity and defect problems, is to model the environment near the defect using a cluster of atoms. This cluster method has achieved accurate results in *ab initio* calculations of the electronic structure of *F*-center defects,[1,2] impurity defects,[3,4] and amorphous materials.[5,6]

An important distinction needs to be made, however, between two different types of cluster calculation. One method uses the infinite crystal potential as the starting point for the defect calculation and alters this potential in the region near the defect to account for its presence. This is a cluster calculation only in the sense that the basis set is constructed using linear combinations of orbitals which are centered about the atoms near the defect. This is, therefore, a cluster in its basis set but not in its potential. It has the advantage that since the potential has the same long-range behavior as that in a perfect crystal, one does not have to worry about any surface effects destroying the bulk environment which should prevail in the region near the defect. One difficulty associated with this technique is that one must ensure that the cluster basis set is orthogonal to all occupied states within the crystal. This is not as difficult in practice as it seems to be at first since one need only orthogonalize to the bulk functions near the defect which overlap strongly with the cluster basis functions. It can become particularly cumbersome for metals, however, since their free-electron behavior causes the defect functions to overlap strongly with a large number of the bulk states.

It is possible for this free-electron behavior to be used to advantage. The main purpose of the previous inclusion of the infinite crystal potential was to prevent the surface of the cluster from affecting the electronic states of the defect. The short screening depth of metals which results from the high mobility of the free electrons would indicate that one might achieve bulk behavior within metals after penetrating a few angstroms into the crystal. This is the basis of a second type of cluster technique which appears to provide an accurate method of obtaining the energies associated with defects in metals. This technique uses the assumption that the environment external to the cluster will be screened from regions of the interior by the free electrons on the surface and that the interior

region will consequently behave essentially as a bulk crystal. Evidence of the validity of this assumption will be provided using comparison of a perfect-crystal bulk density of states with five-shell-cluster results on nickel. Having shown the validity of this assumption we will then present a self-consistent calculation of the energy of a hydrogen atom embedded within a nickel cluster.

II. STRUCTURE AND POTENTIAL

Since, for the present work, the primary objective of the cluster calculation is to provide a host for the hydrogen impurity which has the same properties as the bulk crystal, we placed the nickel atoms in the normal lattice (fcc) arrangement which exists in the bulk nickel crystal. We will begin with a discussion of a pure nickel cluster, in which the origin was centered upon a nickel atom. The cluster was constructed using a central atom with up to five shells of neighboring atoms. Each shell consists of the family of atoms which can be generated by appropriate point-symmetry operations (rotations and/or reflections) on any one of the elements of the shell. Thus, the first shell consists of all nearest neighbors to the central atom and all those rotationally equivalent to the one at $a_0/2(1,1,0)$. Similarly, shell two consists of all points rotationally equivalent to the one at $a_0/2(2,0,0)$, shell three consists of all points rotationally equivalent to the one at $a_0/2$ (2,1,1), shell four consists of all points rotationally equivalent to the one at $a_0/2(2,2,0)$, and shell five consists of all atoms rotationally equivalent to the one at $a_0/2(3,1,0)$. The value of the lattice constant a_0 was taken as the bulk value of 3.52 Å. The electronic charge density used to represent the Coulomb and exchange potentials was obtained from the spin-unrestricted self-consistent band-structure calculation of Callaway and Wang.[7] In order to reduce the complexity of the calculation, we chose to neglect spin polarization and average the spin-up and spin-down states. One would, therefore, expect our results to resemble an average of the spin-up and spin-down results of Callaway and Wang.

The Coulomb potential was obtained from a curve fit of the tabular value of the self-consistent perfect-crystal charge density. This fit was performed using functions centered on each of the atoms as they would occur in a perfect crystal. The form of the Gaussian functions which were placed upon each atom is

$$f(r)=\sum_i \alpha_i \exp(-\beta_i r^2) , \tag{1}$$

where the α's and β's are the linear and nonlinear curve-fit parameters given in Table I. With this expression, the charge density for the cluster is

$$\rho(\vec{r})=\sum_{\vec{R}_v} f(\vec{r}-\vec{R}v) , \tag{2}$$

where f is an atomiclike charge density defined in Eq. (1) and the summation is over all lattice points in the cluster. The Coulomb potential is then given by the conventional expression

$$V(\vec{r})=\int \frac{\rho(\vec{r}')}{|\vec{r}-\vec{r}'|} d\tau' , \tag{3}$$

where the integration is over all space. The double integrals involved in the matrix elements of $V(r)$ in the secular equation can be easily reduced to error functions.[1] Similarly, according to the local exchange approximation, using the Kohn-Sham value of $\frac{2}{3}$, the tabular exchange potential was fitted using Gaussian functions on the atoms of the crystal exactly analogous to Eq. (1). The form of the exchange potential is then

$$V_x(\vec{r})=\sum_{\vec{R}_v} f_x(\vec{r}-\vec{R}v) . \tag{4}$$

The linear and nonlinear curve-fit parameters for this are also given in Table I. The integrals for the

TABLE I. Curve-fit parameters for the nickel cluster.

Charge density	
Linear	Nonlinear
0.134 588	0.328 909
0.775 242	1.246 87
9.497 77	2.647 01
269.853	35.6253
3679.69	591.016
7797.15	4361.43
3137.64	35 000.0
Exchange interaction	
Linear	Nonlinear
0.141 949	0.130 581
0.350 478	0.315 762
1.655 87	1.228 45
5.030 09	23.8237
14.1480	645.009

secular equation corresponding to $V_x(r)$ are three-center integrals of Gaussian functions and are analytic. From these fits one has analytical functions which will give the proper perfect-crystal potential if they were placed upon each of the nickel atoms within the crystal. This should yield the same Coulomb and exchange potential as in the bulk crystal if the cluster is sufficiently large.

It is interesting to examine the accuracy of these curve fits and their effect upon the electronic energies. To study this point we have performed an energy-band-structure calculation for nickel using the standard Fourier techniques while deriving the Fourier coefficients from the same charge density that was curve fitted to get the direct space results. A comparison of the results of these two techniques for various points in the Brillouin zone is found in Table II. The good agreement of these results indicate that our curve fits are accurate enough to produce adequate results for the energy bands.

III. BASIS SET

It has been shown in previous work that one can form an atomiclike basis set which will adequately describe the energy bands of a crystalline solid.[8] This technique involves contracting the single Gaussian basis set to form these orbitals, using the eigenvectors resulting from a perfect-crystal band-structure calculation as combination coefficients. The nonlinear parameters for the single Gaussians were taken from the atomic Hartree-Fock calculation of Wachters.[9] The basis functions for the calculation were constructed from the γ-point ($\vec{k}=0,0,0$) solutions to the band-structure calculation which would correspond, in the free-atomic case, to the $1s$, $2s$, $2p$, $3s$, $3p$, $3d$, and $4s$ states. The linear and nonlinear parameters for each state along with its irreducible representation can be found in Table III. Following the LCAO method, these atomic basis functions were then assigned to each of the atoms of the cluster to form the basis set for the calculation. To reduce the size of the secular determinant, the functions within a given shell of equivalent atoms were combined in correspondence with the irreducible representations of the octahedral group, since the rotational symmetry of the fcc lattice is preserved in the cluster. We further employed the technique of orthogonalized linear combination of atomic orbitals which has had recent success in application to Si III.[5] This involves orthogonalizing the basis set to the core states. A minimal basis set consisting of $3d$ and $4s$ atomiclike functions made orthogonal to the $1s$, $2s$, $3s$, $2p$, and $3p$ atomiclike functions was constructed to determine if it had the variational freedom to represent the lower conduction bands of nickel. A comparison of the energies of the lower conduction states using this minimal basis with that obtained using the full atomic basis is found in Table II. We determined on the basis of this good agreement that the minimal basis set was adequate.

IV. NICKEL CLUSTER

We calculated the electronic states of a nickel cluster consisting of a central atom and five sur-

TABLE II. Comparison of direct space-integration techniques with Fourier space-integration techniques for the energy bands of a perfect crystal of nickel. Investigation into the effect upon the energy bands produced by orthogonalizing the $3d$ and $4s$ functions to the $1s$, $2s$, $3s$, $2p$, and $3p$ atomiclike functions.

	Single Gaussians		Atomic	Orthogonalized to core
	Direct	Fourier	Fourier	Fourier
Γ_1	−0.441	−0.443	−0.443	−0.443
$\Gamma_{25'}$	−0.230	−0.231	−0.231	−0.231
Γ_{12}	−0.194	−0.194	−0.193	−0.193
X_1	−0.300	−0.307	−0.291	−0.291
X_2	−0.169	−0.170	−0.166	−0.166
X_3	−0.287	−0.289	−0.282	−0.282
X_5		−0.162	−0.159	−0.159
L_1	−0.306	−0.309	−0.309	−0.309
L_3	−0.231	−0.232	−0.232	−0.232
		−0.168	−0.166	−0.166

rounding shells of neighboring atoms. The previously described potential and LCAO basis set were assigned to each of the atoms. The density of states (DOS) for this cluster is presented in Fig. 1. The plot is presented as a histogram with the vertical axis in arbitrary units corresponding to the number of states within an energy bin of width 0.005 hartree.

Since the five-shell-cluster results correspond to a finite number of atoms (79) the density of states should contain surface as well as bulk states. It is interesting to investigate these surface states. There are several criteria for their identification. One way to test if a state associated with a particu-

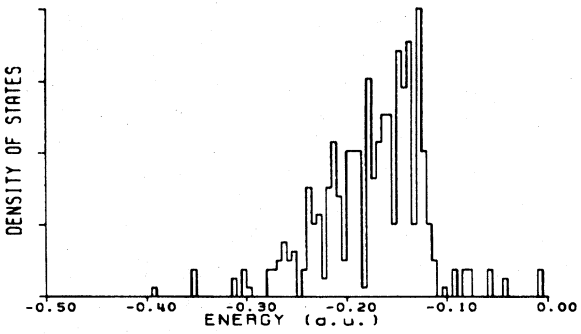

FIG. 1. Full density of states for a five-shell, 79-atom nickel cluster.

TABLE III. Parameters defining transformation from Gaussian to atomic basis set.

1*s*	2*s*	3*s*	4*s*	Nonlinear
0.000 002	0.000 108	−0.001 592	0.079 689	0.130 176
−0.000 148	−0.007 900	−0.376 180	−0.189 834	0.918 169
0.000 768	0.076 833	−0.959 973	−0.423 260	2.394 17
−0.007 323	2.141 93	1.694 55	0.572 429	8.594 00
0.085 595	3.540 87	2.325 74	0.696 224	20.3712
2.968 61	−1.572 67	−0.813 144	−0.228 222	59.2587
11.5979	−6.492 36	−2.611 99	−0.781 217	138.023
18.4070	−7.032 26	−2.844 06	−0.827 086	341.805
17.8700	−6.054 35	−2.334 38	−0.687 908	920.488
13.3509	−4.171 46	−1.628 39	−0.473 567	2761.96
8.688 35	−2.690 06	−1.032 27	−0.302 985	9627.67
5.148 48	−1.567 85	−0.607 356	−0.177 154	41997.9
2.764 33	−0.845 689	−0.325 316	−0.095 257	284878.0
		2*p*	3*p*	Nonlinear
		0.000 808	0.199 436	0.672 528
		−0.009 079	1.506 30	1.710 31
		0.426 812	3.198 25	4.116 25
		7.498 36	−1.667 22	9.928 48
		29.7115	−13.6969	22.387 4
		58.2962	−24.3113	53.1703
		71.0145	−28.4243	138.311
		64.5665	−24.8606	423.403
		49.1666	−18.8644	1774.18
			3*d*	Nonlinear
			0.293 731	0.486 409
			2.661 93	1.574 33
			15.1723	4.639 51
			41.8572	13.7169
			71.0710	48.9403

lar atom was properly screened from the outside (vacuum) environment would be to examine the convergence of the Hamiltonian matrix elements as the contributions to the potential from neighboring atoms are included in the summation. One might expect bulk behavior to occur for atoms which have a sufficient number of neighbors for this convergence to occur. To investigate this we studied the convergence of single-center Hamiltonian matrix elements as a function of the contribution from neighboring atoms to the Coulomb and exchange energies. Both $3d$-$3d$ and $4s$-$4s$ integrals were studied. We found 95% of the Coulomb $3d$-$3d$ and 89% of the $4s$-$4s$ to be accounted for by the single atomic site about which the functions were centered. By including contribution from the twelve nearest neighbors to the atom one could essentially account for all of the Coulomb potential in both cases. The matrix element of the exchange potential, however, does not converge as quickly. The single-atom contribution to exchange was 65% for the $3d$-$3d$ case and 58% for the $4s$-$4s$ case. We found in both cases, however, that the inclusion of the nearest neighbors converged the integrals to within 97% of their final value. It is difficult to study the convergence of the multicenter integrals of this form. However, one would expect by their nature that they would converge more slowly than the single-center ones. One might, therefore, say that the minimum condition for bulk behavior, as far as the electronic energies are concerned, is to have an atom surrounded by its nearest neighbors.

There is another problem, however, with generalizing this to the statement that the wave function of an electron for an atom which is surrounded by all its nearest neighbors would behave the same as in the bulk. This is, of course, due to the fact that in the bulk crystal the wave function is coupled to an infinite-crystal wave function while in the case of a cluster the wave function must be of finite extent. One might say that the convergence of the matrix element is a necessary but not sufficient condition for bulk behavior and that the absolute minimum configuration for bulk states is to have an atom surrounded by its nearest neighbors. For this five-shell cluster, the atoms in the outer shell have six of their twelve possible nearest neighbors. The atoms in the fourth shell have seven nearest neighbors, while those in the third shell have nine nearest neighbors. This might suggest surface behavior for shells four and five with the identity of shell three uncertain.

Another technique, which has been used for the identification of electron states with specific atoms, is Mulliken population analysis.[10] Using this method it is possible to identify the fraction of the contribution to a particular state which corresponds to a given shell within the cluster. One may, therefore, identify surface states as being those which have a large percentage of their electronic wave functions arising from atoms near the surface of the cluster. The local density of states (LDOS) corresponding to those electrons whose wave functions were at least 70% associated with the outer shell is given in Fig. 2(a). We chose the value of 70% as one which might reasonably denote localization of the wave function at the surface. On the same figure [2(b)], we show the density of states corresponding to wave functions consisting of 55% from the outer shell. Comparison of the two plots indicates that, except for a few high-lying states above the Fermi level, the peak is not broadened appreciably. Applying the criteria that surface states should display a sharp LDOS and that they should be spatially localized, a fractional population of at least 55% appears a reasonable condition for identification of a surface state. In Fig. 2(c), we display the LDOS for those states for which there is a combined population in shells four and five of at least 55%. Although the number of states has increased appreciably, the energy distribution has not broadened. This would indicate that our identification of shells four and five as together constituting the cluster surface is supported.

It is interesting to now examine the effects of re-

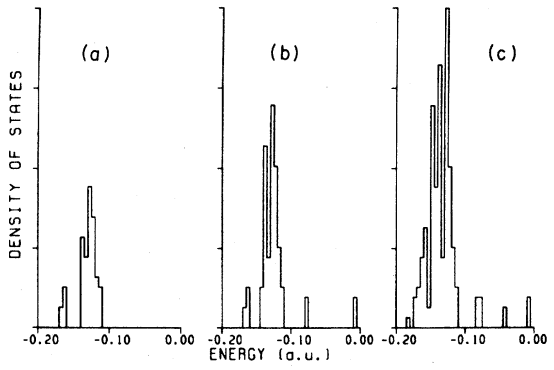

FIG. 2. Local densities of states for the surface of a five-shell nickel cluster. (a) All states with an overlap of at least 0.70 on shell five. (b) All states with an overlap of at least 0.55. (c) All states for which there is a combined overlap of at least 0.55 on shells four and five.

laxing the localization requirement and of including more shells in our surface LDOS. Those states with populations greater than 35% in the outer two shells is displayed in Fig. 3(a). It is not appreciably different from the 55% minimum population requirement of Fig. 2(c), an indication that states associated with the inner shells have little overlap with the surface states, i.e., that the surface states are orthogonal to those in the rest of the cluster. As we include the third shell [Fig. 3(b), 55% combined minimum population], however, we pick up new structure at lower energies which broadens the peak. This broadening comes from atoms which have nine of their twelve possible nearest neighbors. Our identification is that they are essentially bulklike. Those states that we identify as being surface in nature, therefore, occur in a narrow energy range near the Fermi level.

The DOS corresponding to those states remaining after the removal of surface states in Fig. 2(c) is plotted in Fig. 4 together with the bulk density of states for the infinite crystal calculation of Callaway and Wang. Our results are compared with their computation of the density-of-states results for the majority spin carriers instead of their total density of states. Since our total density of states did not include the effects of spin polarization, it was thought that this comparison of states would be more useful than with their total density of states. This comparison is valid under the assumption that the major effect of spin polarization is to cause a rigid shift between the spin-up and spin-down states. Their curve is aligned with ours so that the Fermi levels are coincident. The agreement between the bulk results of the two calculations is seen to be good in light of the different approximations to the starting potential.

Our five-shell-cluster results may also be compared with other cluster treatments of nickel. Messmer and co-workers[11] have performed calculations of the electronic states of a cluster, consisting of a central atom surrounded by a single shell of nearest neighbors using the $X\alpha$ scattered-wave method. The $X\alpha$ calculation was performed self-consistently using a muffin-tin potential, while our calculations used the self-consistent Hartree-Fock bulk potential of Callaway and did not require the muffin-tin approximation. The density-of-states results, for 13-atom clusters, however, are very similar to ours. We compare the DOS for their 13-atom cluster with that for our own 79-atom cluster in Fig. 5. Although the general features are the same, the fine structure is not evident in the $X\alpha$ calculation. The sharp peaks at -0.13 hartree have been identified by us as surface states. When these are removed, the discrepancy is even stronger. This is indicative that a 13-atom cluster is probably too small to achieve a significant degree of bulk screening.

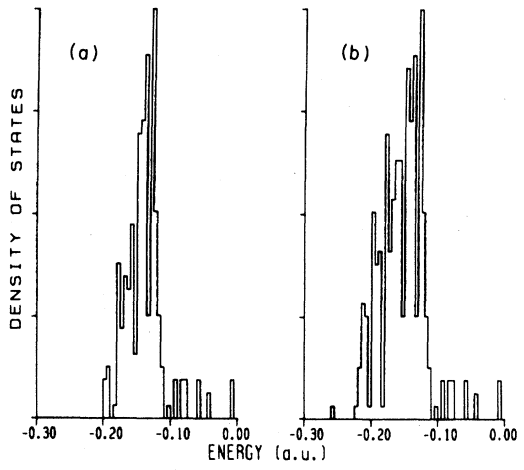

FIG. 3. Local densities of states for a five-shell nickel cluster surface. (a) States with a minimum overlap in shells four and five of at least 0.35. (b) All states with a minimum population of at least 0.55 in shells three, four, and five.

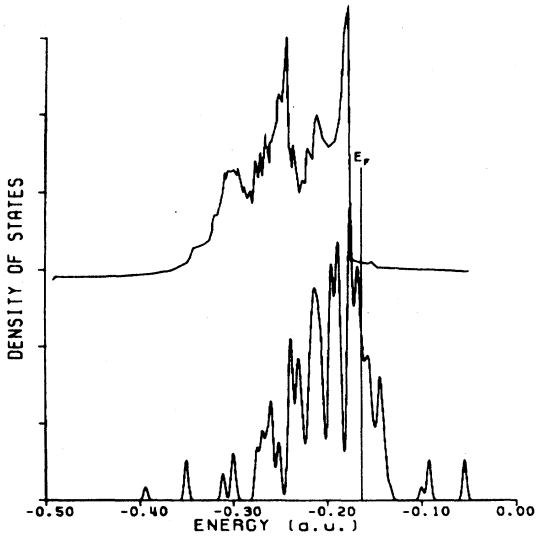

FIG. 4. Comparison of nickel densities of states. Upper curve: infinite crystal DOS for majority spin carriers of Callaway and Wang (Ref. 7). Lower curve: bulk density of states from a five-shell, 79-atom cluster for which the surface states have been removed. E_F represents the Fermi level of both of the plots.

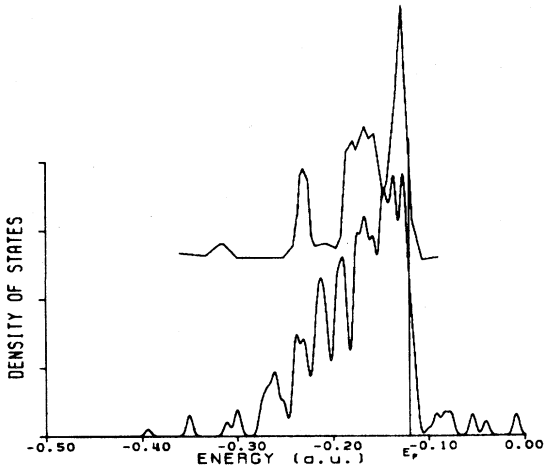

FIG. 5. Comparison of nickel-cluster densities of states. Upper curve: full, one-shell cluster from Messmer *et al.* (Ref. 11). Lower curve: full, five-shell cluster from the present work.

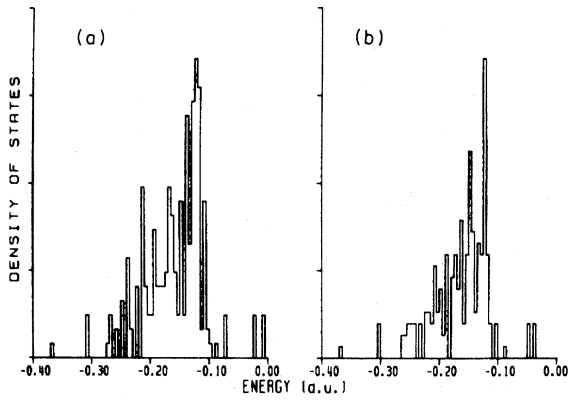

FIG. 6. Nickel-cluster densities of states. (a) Three-shell, 43-atom cluster, centered on a nickel atom. (b) Three-shell, 38-atom cluster centered on an interstitial site.

V. HYDROGEN IN NICKEL

Having established that the internal region of a sufficiently large cluster is essentially equivalent to the bulk crystal, we now have a convenient host environment for the examination of the electronic behavior of impurities in metals. To preserve the rotational symmetry of the nickel cluster we centered the origin upon the hydrogen atom, situated at an interstitial position. A three-shell, 38-atom nickel cluster was then constructed about the interstitial site, placing nickel atoms at the following locations:

(a) Shell one—all atoms rotationally equivalent to the one at $a_0/2(1,0,0)$.

(b) Shell two—all atoms rotationally equivalent to the one at $a_0/2(1,1,1)$.

(c) Shell three—all atoms rotationally equivalent to the one at $a_0/2(2,1,0)$.

It was judged that this configuration was sufficient to screen the central site from the vacuum environment.

Since the origin of the center of rotation of this cluster is different from that of the previously defined five-shell cluster, one might expect a different density of states from that produced by an equivalent number of atoms with a different center of rotation. If one were truly in a bulk crystal, however, a shift in origin should not affect the density of states. Agreement between the density of states for clusters corresponding to different centers is, therefore, a necessary condition for the clusters to behave as bulk. One should expect that these two different clusters would give very similar density of states. The density of states corresponding to a 38-atom pure nickel cluster, centered about an interstitial site with that of a 43-atom cluster (three shells) centered on a nickel atom are presented in Fig. 6. One sees that there is excellent agreement between the two results, everywhere except at the top of the band where the surface states reside. This agreement is, of course, a necessary requirement for the clusters to have a bulk nature.

To evaluate the properties of a hydrogen impurity in nickel, it is necessary to add to the potential of the previously described 38-atom nickel cluster, the nuclear, Coulomb, and exchange contributions for the hydrogen atom. This was done in a manner similar to the way in which the nickel-cluster potential was constructed. As a first approximation, the charge density corresponding to a free atom of hydrogen was placed at the central interstitial site of the cluster. This charge density was treated as a difference between the hydrogenated cluster and the charge density of the pure nickel cluster. It was curve fitted using Gaussians, with the added constraint that the total charge corresponding to the fit of the difference be one electronic charge, forcing the fit to preserve the charge neutrality of the cluster. We found that the region near the hydrogen atom was the only part of the cluster which was significantly altered by the presence of hydrogen and that an acceptable fit could

be obtained using Gaussians centered on the hydrogen atom. The form of the Gaussian functions placed upon the hydrogen atom is the same as Eq. (1). The exchange potential was approximated by curve fitting the difference between the exchange potential corresponding to a nickel cluster with hydrogen impurity and one corresponding to the pure nickel cluster. Since this difference is a result of the additional charge associated with the impurity, it is a localized function and can be fitted using Gaussians centered on the hydrogen atom. The form of the Gaussian functions placed on the hydrogen atom is also the same as Eq. (1).

This calculation was then iterated to self-consistency according to the following procedure. The eigenvectors from the previous iteration were used to construct the charge density for all regions within the hydrogenated cluster. This charge density was compared with the original charge density corresponding to the pure nickel cluster and it was again found that significant difference from this pure nickel charge density occurred only in the region near to the hydrogen atom. We, therefore, fit this charge-density difference using functions centered about the hydrogen. Since the difference in charge density was localized the difference in the exchange potential was also localized and could be fitted using Gaussian functions centered about the hydrogen atom. The Gaussian fits of the charge density and exchange potential resulted in the proper modifications to the pure-nickel-cluster potential required for the next iteration. The linear and nonlinear parameters for the Gaussian coefficients of the self-consistent Coulomb and exchange potential are given in Table IV. Self-consistency was achieved at the end of four iterations. The density-of-states results for a self-consistent hydrogenated cluster may be found in Fig. 7(a). They may be contrasted with the density of states of an equivalent pure nickel cluster in Fig. 7(b). If one compares these two plots it is found that the main effect of the addition of the hydrogen is to introduce a state at -12.95 eV and to shift upward the states at the bottom of the Ni band.

Energy band-structure results have been obtained for nickel hydride by Switendick.[12] Comparison can be made of our density-of-states results with those of the nickel hydride perfect crystal. Two major differences in the structure should lead to differences in the density of states. The first difference is a result of the fact that our finite cluster will have both surface and bulk states in the DOS plot. We used the Mulliken population-analysis technique described previously to remove those surface states which were at least 55% associated with the outer shell (shell three) from our density-of-states plot. The second difference is that nickel hydride corresponds to a much higher concentration of hydrogen in the nickel crystal than we construct in our calculation of a single hydrogen atom in a 38-atom cluster. One might expect that the first-order effect of this difference would be that the additional hydrogen atoms would interact with each other to broaden the peak

TABLE IV. Curve-fit parameters for hydrogen.

Charge density	
Linear	Nonlinear
−0.002 822	0.100 000
0.172 514	0.299 587
−0.596 331	0.499 542
1.658 34	0.998 613
−1.810 81	1.504 92
0.852 651	2.437 15
0.052 580	18.0696
Exchange interaction	
Linear	Nonlinear
0.898 717	0.299 324
−2.845 44	0.499 865
7.450 18	1.000 29
−10.5170	1.508 42
5.741 35	2.003 36
−0.347 493	4.049 71
0.048 792	13.0023

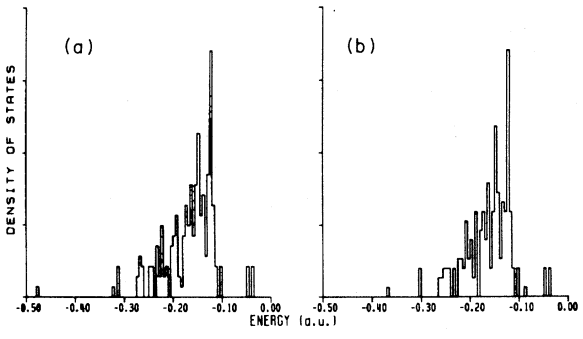

FIG. 7. (a) Three-shell, 38-atom nickel cluster with a hydrogen atom occupying the central, interstitial site. (b) Same cluster without hydrogen impurity.

we obtain at -12.95 eV. This is indeed the case as one observes in our comparison with his results (Fig. 8). Notice that there is good agreement between the two plots and that the essential features are the same aside from a broadening of the lower peak.

Calculation of the electronic structure of a hydrogen atom embedded within nickel clusters has been performed using the $X\alpha$ scattered-wave method by Messmer *et al.*[13] They performed two calculations—one for a hydrogen atom surrounded by four nickel atoms in tetrahedral coordination and a second for a hydrogen atom surrounded by six nickel atoms at the normal bulk structure locations. They provided density-of-state information solely for their four-nickel-atom cluster. A comparison of the DOS of their hydrogenated four-atom cluster with our hydrogenated 38-atom cluster is found in Fig. 9. These two results are compared by equating their Fermi energies. The qualitative features of the two calculations are in agreement. The appearance of a low-lying state and the shift upward of the lower conduction-band state with the introduction of hydrogen is also found in their work. Our nickel bands are, however, wider than theirs and the position of the lower hydrogen-induced energy state is farther below the Fermi energy. The wider bands appear with the inclusion of additional atoms as evidenced by the density of states for the $X\alpha$ atom cluster in Fig. 5. We also did not observe a shift in Fermi energy associated with the addition of the hydrogen atoms to the Ni cluster which was described in the four- and six-atom-cluster work. This is another indication that our 38-atom cluster was essentially bulk-like since the presence of a hydrogen atom should not affect the bulk Fermi energy in a nickel crystal.

The primary effect of the presence of the hydrogen atom is to interact with the state at -9.96 eV corresponding to the bottom of the conduction band to produce a lower-energy state at -12.96 eV and a higher state at -8.82 eV. It is interesting to investigate, using Milliken's population analysis, the character of this lower-energy state. It corresponds to the Γ_1 or A_{1g} irreducible representation and therefore has full rotation symmetry about the hydrogen atom. Its constituents are 42% of s-type functions about the hydrogen atom, 44% $4s$ functions, and 14% $3d$ functions from the nearest-neighbor nickel atoms. There was a negligible contribution from nickel atoms at outer shells. Since according to the spin-restricted Hartree-Fock-Slater method, each electronic state must be occupied by two electrons, one may consider that the one electron associated with a free hydrogen atom has been reduced to about 0.84 when the hydrogen is in nickel. This result gives some quantitative justification for the picture of hydrogen entering a nickel crystal essentially as a neutral atom and not ionizing. A plot of the difference in the electronic charge density between the pure nickel cluster and the hydrogenated nickel cluster is found in Fig. 10. The plot is along the (1,0,0) direction toward the nearest-neighbor nickel atom. A plot of the free-

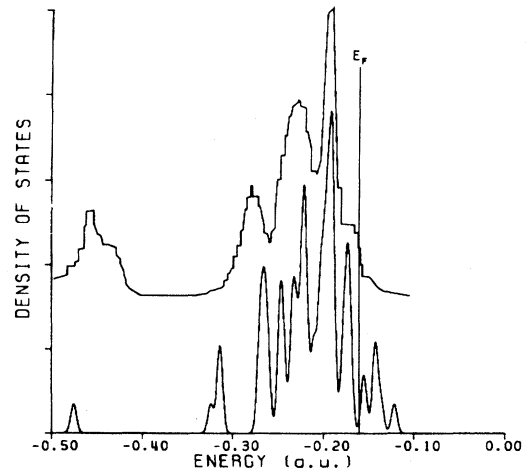

FIG. 8. Comparison of hydrogenated nickel bulk densities of states. Upper curve: NiH bulk calculation of Switendick (Ref. 12). Lower curve: 38-atom cluster with surface states removed and single hydrogen atom occupying the central, interstitial site. E_F represents the Fermi level of the cluster.

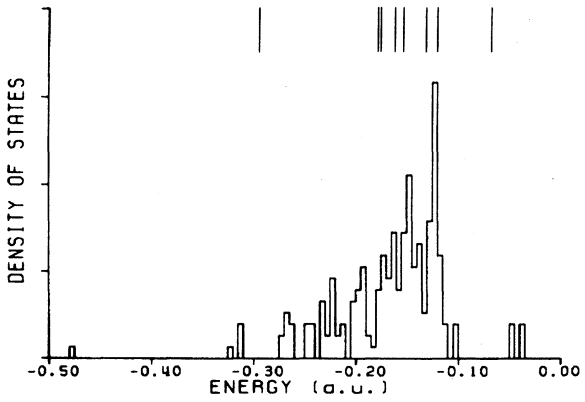

FIG. 9. Comparison of hydrogenated nickel cluster densities of states. Upper lines: central hydrogen atom with four neighboring nickel atoms in tetrahedral coordination (Ref. 13). Lower lines: full 38-atom cluster with centrally located hydrogen impurity.

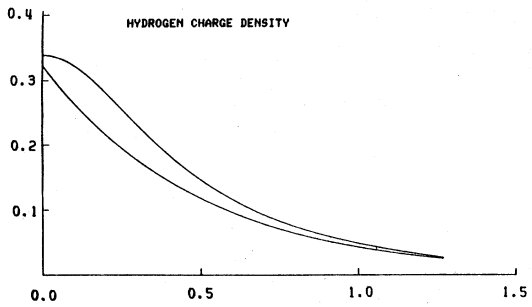

FIG. 10. Upper curve: difference in charge density between hydrogenated and pure nickel cluster. The origin is at the central interstitial site. Lower curve: free-atomic charge density from a 1*s* hydrogen electron. Plot is in atomic units.

hydrogen charge density is also provided in the figure (lower curve) for comparison. Notice that there is a great deal of similarity between the two curves, the primary difference being at the origin, near the proton, giving further justification to the neutral hydrogen picture for hydrogen in nickel.

The primary difference between the two curves of Fig. 10 is in the region near to the proton. The difference charge density appears to be less sharp in this region than the neutral-atom charge density. One might wonder whether we included enough variational freedom in our charge-density functions to represent a sharp feature like the free-hydrogen charge density. If we had not, one could argue that the difference between the two curves is a result of the lack of variational freedom. To investigate this point we performed a linear curve fit of the free-atom charge density using the Gaussian functions of Table IV. The only difference between the free-atom charge density and the fit occurred in the region from the proton out to a radius of 0.06 a.u. Since this region represents a very small fraction of the volume for which the curves in Fig. 10 differ, we concluded that this difference was a physical effect and not a numerical artifact.

VI. CONCLUSION

It has been previously indicated that small metallic clusters provide an environment which approximates that of the bulk crystal.[11] Our work demonstrates, however, that a cluster of at least three shells of atoms is required to obtain quantitative agreement with bulk calculation. Using the LCAO technique with direct-space integration one can conveniently handle these larger clusters and use them as a model for the investigation of the properties of defects in metallic solids.

Mulliken population analysis provides a useful tool in the identification of the surface states of the cluster, although it is not as easy to identify these states in a metal as it is in insulators. The surface states do seem to occupy a narrow band near the Fermi level.

The hydrogen-defect calculation agrees with a qualitative picture of the hydrogen atom going into the nickel crystal as a neutral atom and not appreciably ionizing. The energy level associated with the hydrogen atom occurs at -13.0 eV which is not far from the free-hydrogenic value of -13.6 eV.

The absolute position of the Fermi energy for the cluster is shifted by 0.4 eV to a value of -3.3 eV as the cluster size increased from a central atom plus two shells to a central atom plus five shells. An even more drastic shift in the Fermi energy occurred upon removal of states associated with the cluster surface (see Fig. 4). The Fermi level for Fig. 4 corresponds to a value of -4.6 eV and compares favorably with the experimental work function of about 5.2 eV.[14] However, since it appears that the absolute position of the Fermi level is very sensitive to the cluster size and to the identification of surface states within the cluster, we would not place a lot of significance to this favorable agreement.

The LCAO method, using direct-space integration techniques, seems to be a convenient approach for studying metallic clusters. It allows the evaluation of all the matrix elements analytically subject to the local exchange approximation. No approximation of the form of the potential is necessary to conveniently perform the calculation. It is computationally tractible to use this method to study clusters of the size of hundreds of atoms. The technique seems to be particularly useful in application of defects in metals, since the bulk properties in a metal can be achieved by using clusters of about 40 atoms.

ACKNOWLEDGMENT

This work was supported in part by the University of Texas at Dallas Organized Research Fund.

[1]R. C. Chaney and C. C. Lin, Phys. Rev. B 13, 843 (1976).
[2]R. C. Chaney, Phys. Rev. B 14, 4579 (1976).
[3]J. G. Harrison and C. C. Lin, Phys. Rev. B 25, 3894 (1981).
[4]R. W. Simpson, N. F. Lane, and R. C. Chaney, J. N. Materials 69&70, 581 (1978).
[5]W. Y. Ching and C. C. Lin, Phys. Rev. B 12, 5536 (1975).
[6]W. Y. Ching, J. G. Harrison, and C. C. Lin, Phys. Rev. B 15, 5975 (1977).
[7]J. Callaway and C. S. Wang, Phys. Rev. B 7, 1096 (1973).
[8]J. E. Simmons, C. C. Lin, D. F. Fouquet, E. E. Lafon, and R. C. Chaney, J. Phys. C 8, 1594 (1975).
[9]A. J. H. Wachters, J. Chem. Phys. 52, 1033 (1970).
[10]R. S. Mulliken, J. Chem. Phys. 23, 1833 (1955); 23, 1841 (1955); 23, 2338 (1955).
[11]R. P. Messmer, S. K. Knudson, K. H. Johnson, J. B. Diamond, and C. Y. Yang, Phys. Rev. B 13, 1396 (1976).
[12]A. C. Switendick, Ber. Bunsenges. Phys. Chem. 76, 535 (1972).
[13]R. P. Messmer, D. R. Salahub, K. H. Johnson, and C. Y. Yang, Chem. Phys. Lett. 51, 84 (1977).
[14]W. Eib and S. F. Alvarado, Phys. Rev. Lett. 37, 444 (1976).